



Evaluation of the Performance of TiO₂-CeO₂ Bilayer Coatings as Photoanodes for Corrosion Protection of Copper

Raghavan Subasri,^{a,*} Sameer Deshpande,^{b,**} Sudipta Seal,^b and Tadashi Shinohara^a

^aCorrosion Group, Materials Information Technology Station, National Institute for Materials Science, Tsukuba 305-0047, Japan

^bAdvanced Materials Processing and Analysis Center, Mechanical, Materials, Aerospace Engineering, University of Central Florida, Orlando, Florida 32816, USA

Bilayer coatings consisting of a CeO₂ inner layer and a TiO₂ outer layer were made on copper substrates (Cu|CeO₂|TiO₂) and the photoelectrochemical properties of the derived bilayered photoelectrodes for corrosion protection application was investigated and compared with the performance of our previously studied Sb-SnO₂-TiO₂ bilayered photoelectrodes coating for similar applications. TiO₂ and CeO₂ sols were used for preparing the coatings. Investigations on the charge storage capacity of the two different bilayered coatings revealed that the Sb-SnO₂-TiO₂ system is capable of storing higher charge at less negative applied potentials, i.e., -600 mV vs SCE, whereas, the CeO₂-TiO₂ system stores higher charge at more negative applied potentials, i.e., -900 mV vs SCE.

© 2005 The Electrochemical Society. [DOI: 10.1149/1.2133723] All rights reserved.

Manuscript submitted August 3, 2005; revised manuscript received August 20, 2005. Available electronically November 18, 2005.

Copper has been proposed as the ideal material for construction of canisters to be used for the disposal of spent nuclear fuels because of its outstanding corrosion resistance, ease of fabrication, abundant availability, and overall cost-effectiveness. For these reasons, extensive research has been pursued for assessment of suitability of copper for these same purposes and, therefore, corrosion protection of copper in the conditions prevailing underground becomes a matter of concern because the passive and protective copper oxide layer does not form when the oxygen potentials are very low. In this context, cathodic protection offered by TiO₂ in the presence of ultraviolet (UV) light could be envisaged as appropriate. There have been substantial efforts to exploit the photocatalytic applications of nano TiO₂ in all fields that it is predicted to become a part of every individual's life in a few years. One of the most promising applications that has stimulated considerable interest in the recent past is its use as a photoanode for corrosion protection of metal and steel substrates. The working principle of photoaided cathodic protection is that when a metal coated with a thin layer of TiO₂ is exposed to UV irradiation, e⁻-hole pairs are created in the TiO₂ layer. The photogenerated electrons can be transferred to the metal substrate thereby making its electrode potential more negative than its corrosion potential. The main advantage of this method is that the photoanode, i.e., TiO₂ in this case, does not get consumed during the process of corrosion protection, unlike a sacrificial-type cathodic protection. However, in the case of the applicability of TiO₂ coatings for corrosion protection of copper under subterranean conditions, there would be no light available for such a purpose. But this problem is not a serious one as the containers would hold high-level nuclear waste and the gamma radiation being emitted from them could itself be visualized as an in situ source of UV illumination, provided suitable radiation converters are incorporated in the protective TiO₂-based coating. The exact mechanism of corrosion protection offered by a TiO₂ coating on metal/steel substrate in presence of UV illumination has been discussed in detail in Refs. 1-4.

One of the inherent disadvantages of using a plain TiO₂ coating for anticorrosion applications is that the photoeffect ceases to be operative once the UV illumination stops shining on the TiO₂-coated substrate. A possible method for solving this problem would be to couple another semiconductor like SnO₂ whose conduction band (CB) level is lower than that of TiO₂⁵ so that the photo-

generated electrons could be transferred from TiO₂ to SnO₂ and the coupled semiconductor, i.e., SnO₂, should be capable of storing and releasing the photogenerated electrons. Another candidate semiconductor that could be coupled with TiO₂ would be nano CeO₂. There are several reports on the use of CeO₂-TiO₂ electrodes for electrochromic windows, where the reversibility for lithium insertion in CeO₂ was used for transmissive electrochromic devices.^{6,7} In addition, a recent report describes the application of hierarchically mesostructured CeO₂ for use in solar cells,⁸ where the active component is nanometric ceria using a constructed organic-dye-free solar cell. The reason for this is that the bandgap of nanometric ceria was found to have shifted by 80 nm when compared to that of TiO₂. In view of the potential applications of nanocerium, the present investigation was carried out with an objective to measure the photoelectrochemical properties of TiO₂-CeO₂ bilayer electrodes on copper substrates and to find out if such electrodes possess the desirable properties of an efficient photoanode for corrosion protection. The results obtained are compared with the performance of the Sb-SnO₂|TiO₂ electrode for the same application.

Experimental

Synthesis.— A commercial 4 wt % TiO₂ sol solution (pH 7.0) supplied by Nihon Parkerizing Co., Ltd., Japan, was used as the source of TiO₂. The average crystallite size of TiO₂ in the solution was ~10 nm. Ceria nanoparticles were synthesized using a low energy wet chemical synthesis technique known as microemulsion, the details of which are given as follows. The microemulsion system consists of surfactant sodium bis(2-ethylhexyl)-sulfosuccinate (AOT), toluene, and Millipore DI water. All the chemicals were purchased from (Aldrich, Inc.). AOT was dissolved in toluene and 0.1 M aqueous cerium nitrate solution was added. The mixture was stirred, and hydrogen peroxide was then added dropwise. The detailed synthesis procedure is explained in Ref. 9. The reaction was carried out for 2 h and then the reaction mixture was allowed to separate into two layers. The upper, pale yellow layer was toluene-containing nonagglomerated ceria nanoparticles and the lower layer was the aqueous phase. The morphology of CeO₂ nanoparticles was studied by high resolution transmission electron microscopy (HRTEM) using a Philips HRTEM operated at 300 kV accelerating voltage. Figure 1 shows the HRTEM image of the synthesized cerium oxide nanoparticles.

Copper specimens of dimensions 3 × 2 × 0.1 cm were used as the substrates. The copper plates were polished to a mirror finish with 0.05 μm Al₂O₃ prior to coating and thoroughly degreased in acetone for 5 min in an ultrasonic cleaner, which were subsequently used as substrates for coating the photoanode material. The photo-

* Electrochemical Society Active Member.

** Electrochemical Society Student Member.

^c Present address: International Advanced Research Centre for Powder Metallurgy and New Materials, Balapur, Hyderabad 500 005, India.

^z E-mail: subasri@arci.res.in

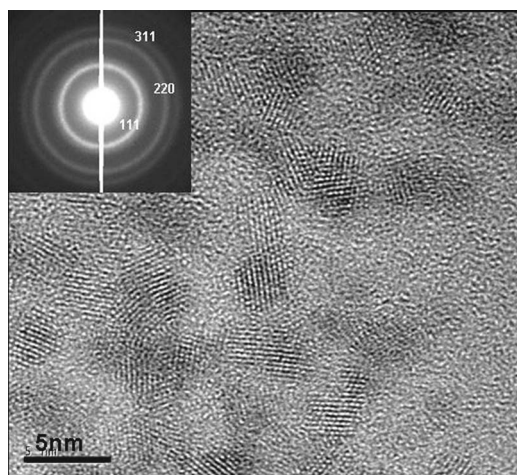


Figure 1. HRTEM image of nanoceria particles (size 2–5 nm). (Inset shows the SAED pattern indicating the fluorite structure of nanoceria sample.)

anode coating consisted of two layers, the first one being CeO_2 and the outer layer TiO_2 . CeO_2 coatings on copper coupons were made using a dip coater, and the coating thickness was calculated using the weight difference of coupons before and after coating. The coating thickness was approximately 300 nm on each sample. TiO_2 coatings on the CeO_2 layer were made by the spin-coating technique in order to achieve a thickness of ~ 200 nm for the TiO_2 layer. The total thickness of the photoanode was measured to be approximately 500 nm. The bilayered photoelectrode coating on the copper substrate was co-fired at 200°C for 20 min in a N_2 atmosphere to obviate oxidation of copper during heating. The heat treated coupons were subsequently subjected to photoelectrochemical characterization.

Photoelectrochemical characterization.— Electrochemical characterization was carried out by measuring the open circuit potential (OCP) of the samples under dark and UV illuminated conditions with reference to a saturated calomel electrode (SCE). A deaerated 0.3% NaCl solution was used as the electrolyte unless otherwise mentioned, and a Pt strip was used as the counter electrode for polarization measurements. In order to simulate the conditions prevailing underground, a deaerated atmosphere was created during the electrochemical studies by purging the electrolyte solution with N_2 (purity, 99.9%). A 500 W Hg lamp was used as the source of UV illumination. The light first passed through an optical filter (UV-34, Kenko), which mostly ($>60\%$) allowed only light of wavelengths greater than 340 nm. After this light passed through a quartz window, it was then made to fall on the coated side of the copper plate. A transparent electrochemical cell made of acryl fitted with a quartz window on one side was used. The sample was fixed on the opposite side with the aid of an O ring. A more detailed description of the experimental details is given in Ref. 10.

For impedance measurements, the same conditions with respect to atmosphere and electrolyte as used for the OCP measurements were maintained. Impedance was measured as the current response to a superimposed ac signal of amplitude 20 mV with a frequency ranging from 0.01 Hz up to 1 kHz at various applied potentials provided by a potentiostat, model 2090 HS supplied by Toho Techniques Research, Japan. After a preliminary analysis of the impedance data obtained for various applied potentials as a function of frequency, it was found that at lower frequencies (<0.1 Hz), the system showed a capacitive behavior, and this was ascertained to be arising from the bilayer electrode coating. Hence, for measurement of the capacitance of the coating, the impedance was measured at potentials ranging from -100 mV down to -1150 mV in steps of 50 mV at a low frequency of 0.01 Hz. The system was kept for

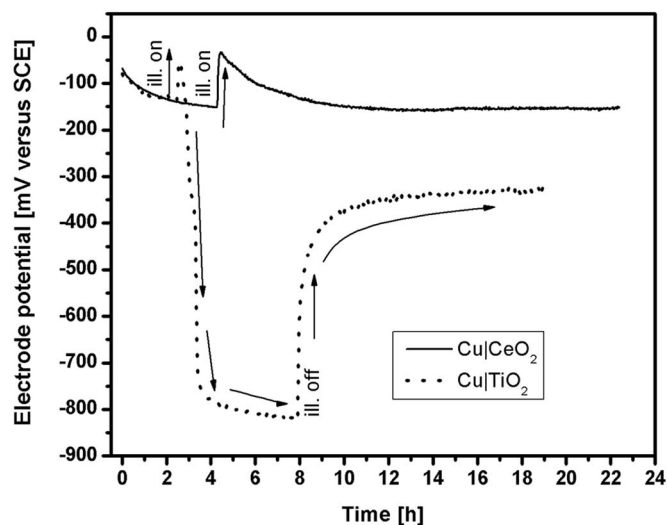


Figure 2. Comparison of the response of electrode potentials to UV illumination for $\text{Cu}|\text{CeO}_2$ and $\text{Cu}|\text{TiO}_2$.

45 min at any applied potential before measurement, as it was verified that a constant current state was reached at 45 min after application of potential.

Results and Discussion

As a first step, the response of the OCP of different samples to UV illumination was studied and their time evolution observed after exposure to UV source and after cutting it off.

Figure 2 shows the time evolution of the OCP on exposure to UV illumination for $\text{Cu}|\text{CeO}_2$. It can be seen that there is an initial p-type effect (OCPs instantaneously becoming more positive) on exposure to UV light. But after sometime, the electrode potential slowly reverts back to negative values. Nevertheless, the values do not become more negative than -180 mV whereas, in the case of a plain TiO_2 coating (also included in Fig. 2), though the same initial p-type effect is observed, after some time, the electrode potentials slowly become more negative and finally reach values of -800 mV, which is the photopotential of TiO_2 . The initial p-type effect is due to the presence of a thin layer of copper oxide ($\text{Cu}_2\text{O}/\text{CuO}$) present between the copper and the semiconductor oxide coating, that could have formed due to the interaction of the copper surface with the water-based sol solution during heat-treatment. Cu_2O and CuO are both p-type semiconductors with bandgap equal to 2 and 1.2 eV, respectively, and their presence adversely affects the normal n-type photoeffect in TiO_2 as shown in Fig. 2. The copper oxide layer can be reduced by photogenerated electrons from TiO_2 ,¹⁰ but the photoeffect in CeO_2 , though capable of reducing the copper oxide layer, cannot make the OCP reach large negative values like TiO_2 (cf. Fig. 2). Hence, there is a necessity to include TiO_2 in the photoanode containing CeO_2 . But since the electrical conductivity of CeO_2 is greater than that of TiO_2 , the design of a bilayer coating was thought of, where the photoeffect could be generated by an outer TiO_2 layer, from which the photogenerated electrons could be passed on to the substrate via an intermediate CeO_2 layer, whose electrical conductivity was substantial to facilitate charge transfer. In addition, since CeO_2 is also capable of exhibiting multiple valence, it is expected to store charge in the form of photogenerated electrons according to Eq. 1, which will sustain the photoeffect even after cessation of UV illumination, by releasing the stored electrons to the substrate



where $M = \text{H}$ or Li and $x = 1$.

Figure 3 depicts a comparison of the response of the OCP response on exposure to UV illumination for the $\text{Cu}|\text{CeO}_2|\text{TiO}_2$ which

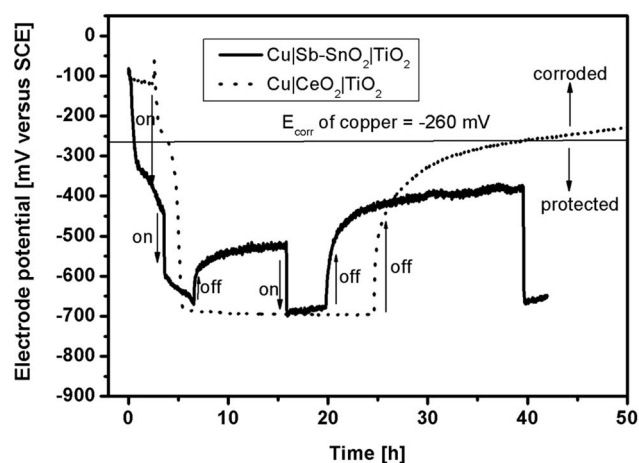


Figure 3. Time evolution of electrode potential and its response to UV illumination compared for Cu|CeO₂|TiO₂ and Cu|Sb-SnO₂|TiO₂.

is also compared with that of Cu|Sb-SnO₂|TiO₂ (taken from Ref. 10). It can be seen that, though both the profiles are comparable with respect to the absolute values of the photopotentials, the recovery of the electrode potentials after the source of UV illumination has been cut off, differs to a slight extent. The electrode potential after the stopping of illumination is more negative for the bilayer electrode containing Sb-SnO₂ than that obtained in the case of CeO₂ and remains at such values for a longer period of time. This clearly indicates that the charge-storage property of Sb-SnO₂ is different from that of CeO₂, which result is expected. The charge-storage property could be quantified by measuring the capacitance as a function of applied voltage, which was carried out by measuring the impedance at low frequencies such as 0.01 Hz, with varying applied potentials.

Figure 4 shows the Bode plot for the sample polarized at -600 mV vs SCE. An equivalent circuit corresponding to the configuration given in Fig. 5a was assumed for the analysis of the impedance data. The impedance information can be divided into three distinct regions. R_s represents the solution resistance (appears at very high frequencies); R_H, C_H are those from the high frequency response (due to electrode solution interface); R_L, C_L are the resistance and capacitance components of the low frequency response (due to the semiconductor oxide coating). The value of each component was determined from the absolute value of the impedance determined at specific frequencies where only one of the compo-

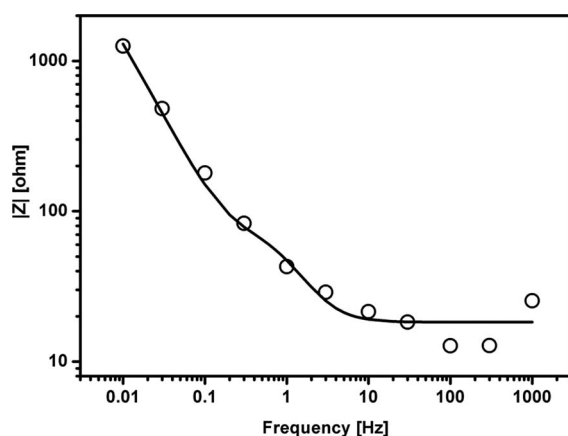


Figure 4. Impedance measured as a function of frequency for the 200°C HT Cu|bilayered electrode at an applied potential of -600 mV vs SCE; solid line is the curve fitting according to equivalent circuit given in Fig. 5a.

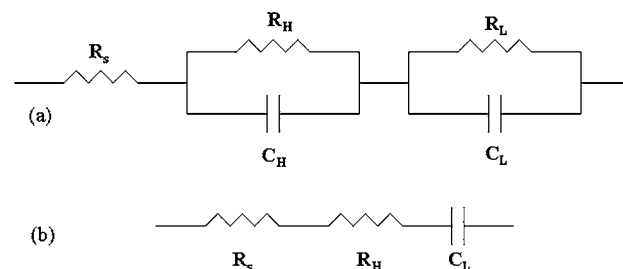


Figure 5. (a) Equivalent circuit proposed conforming to the measured impedance data and (b) reduced circuit at low frequencies.

nents would be a major contributor to the total impedance, neglecting the effect due to others. The calculated data assuming the equivalent circuit fitted well with the measured data and is shown as a solid line in Fig. 4.

From the impedance measurements at 0.01 Hz for various applied potentials, the capacitance of the bilayer coating was determined at each applied potential at this frequency assuming the equivalent circuit shown in Fig. 5b and plotted in Fig. 6. Figure 6 shows a comparison of the capacitance for Cu|TiO₂, Cu|Sb-SnO₂|TiO₂, and Cu|CeO₂|TiO₂ samples measured as a function of the applied electrode potential vs SCE. The Cu|TiO₂ electrode obviously stores less charge throughout the range of applied potentials of measurement when compared to the other two electrodes. This is due to the fast charge recombination (electron-hole) on the TiO₂ surface. However, when one compares the charge-storage property of Cu|Sb-SnO₂|TiO₂ and Cu|CeO₂|TiO₂, it is seen that Sb-SnO₂ exhibits a constant charge, i.e., 3500 $\mu\text{F}/\text{cm}^2$ stored over potentials from -400 mV down to -700 mV and then there is a sudden increase in the amount of charge stored for still lower potentials. The large values of capacitance at $E_{\text{app}} = -600$ mV corresponds to the one electron reduction from Sn⁴⁺ to Sn³⁺ followed by subsequent reduction to Sn²⁺ as indicated by the sudden increase in the capacitance beyond $E_{\text{app}} = -800$ mV. The high capacitance values of ~ 2000 $\mu\text{F}/\text{cm}^2$ at $E_{\text{app}} = -600$ mV confirm that when the electrode potential reaches the value of -600 mV during illumination (photopotential), there is a charging up of the electrode. When the source of illumination is cut off, this stored charge is slowly discharged to the substrate such that a highly negative electrode potential of the substrate is still maintained.

In the case of Cu|CeO₂|TiO₂ there is low charge ranging from 150–550 $\mu\text{F}/\text{cm}^2$ stored at potentials from -450 down to -700 mV and then there is a sudden increase in the stored charge, which is even higher than that stored by the Sb-SnO₂|TiO₂ electrode at even

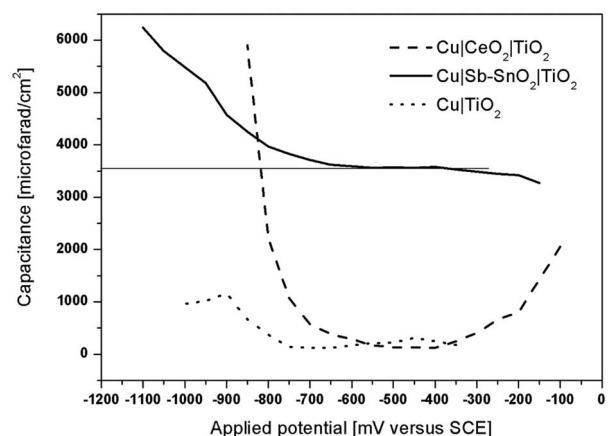


Figure 6. Capacitance as a function of applied potential for Cu|CeO₂|TiO₂ and Cu|Sb-SnO₂|TiO₂.

potentials. This indicates that the reduction of Ce^{4+} to Ce^{3+} takes place at a more negative electrode potential when compared to Sn^{4+} reduction.

It is desirable that the reduction of the multivalent species (Sn^{4+} or Ce^{4+}) in the photoanode should take place at its photopotential, so that the photogenerated electrons can be transferred from TiO_2 and can be stored simultaneously. In view of this requirement, from the present study, it can be inferred that the $\text{Cu}|\text{Sb-SnO}_2|\text{TiO}_2$ electrode is preferable as a photoanode when compared to $\text{Cu}|\text{CeO}_2|\text{TiO}_2$. However, the $\text{CeO}_2|\text{TiO}_2$ electrode could also be made more efficient, if the photopotentials can be made around -800 mV, where an in situ reduction of Ce takes place and the charge can be reversibly stored and released to the substrate, thereby sustaining the photoeffect.

Conclusion

The present study was carried out to evaluate and compare the performance of $\text{Cu}|\text{CeO}_2|\text{TiO}_2$ bilayered photoelectrode with $\text{Cu}|\text{Sb-SnO}_2|\text{TiO}_2$. The photoelectrochemical properties were characterized by measuring the electrode potential response to UV illumination and the charge-storage capacity by impedance measurements as a function of applied electrode potential. The investigations revealed that $\text{Cu}|\text{Sb-SnO}_2|\text{TiO}_2$ bilayered photoelectrode showed

good charge-storage capacity at the photopotential of TiO_2 . Nevertheless, the results also showed that if the photopotential of the electrode could be made -800 mV or lower, $\text{Cu}|\text{CeO}_2|\text{TiO}_2$ bilayered photoelectrode is also capable of very high charge storage.

Acknowledgment

R.S. acknowledges the National Institute for Materials Science, Tsukuba, Japan, for financial support in the form of a fellowship.

National Institute for Materials Science assisted in meeting the publication costs of this article.

References

1. J. Yuan and S. Tsujikawa, *J. Electrochem. Soc.*, **142**, 3444 (1995).
2. J. Huang, T. Shinohara, and S. Tsujikawa, *Zairyo Kagaku*, **46**, 789 (1997); *Zairyo Kagaku*, **46**, 651 (1997).
3. Y. Ohko, S. Saitoh, S. Tatsuma, and A. Fujishima, *J. Electrochem. Soc.*, **148**, B24 (2001).
4. H. Park, K. Y. Kim, and W. Choi, *J. Phys. Chem.*, **106**, 4775 (2002).
5. R. Subasri and T. Shinohara, *Electrochem. Commun.*, **5**, 897 (2003).
6. P. Baudry, A. C. M. Rodrigues, and M. A. Aegerter, *J. Non-Cryst. Solids*, **121**, 319 (1990).
7. Q. N. Zhao, C. L. Li, and X. J. Zhao, *Key Eng. Mater.*, **249**, 451 (2003).
8. A. Corma, P. Atienzar, H. Garcia, and J. Y. C. Ching, *Nat. Mater.*, **3**, 394 (2004).
9. S. Patil, S. C. Kuiry, S. Seal, and R. Vanfleet, *J. Nanopart. Res.*, **4**, 433 (2002).
10. R. Subasri, T. Shinohara, and K. Mori, *J. Electrochem. Soc.*, **152**, B105 (2005).